A Novel FEF Method for Insulation Status Monitoring of Underground Power Cables

Songyi Dian
School of Electrical Engineering and Information Technology,
Sichuan University, Chengdu, China
Email: scudiansy@scu.edu.cn

Mengyu Liang, Bingwu Lou and Tao Liu
School of Electrical Engineering and Information Technology,
Sichuan University, Chengdu, China
Email: arsenal630919@yahoo.com.cn, louby53@sina.com, favmoon@hotmail.com

***Abstract*—Monitoring on underground power cables in a close-fitting manner using mobile robot can acquire more actual information about insulation status of cables. Focusing on a water tree detection module in the monitoring system, this paper proposes fringing electric field (FEF) method to detect probably formed water tree in the insulation layer. An arch substrate based interdigital FEF sensor is designed to reduce the disturbance caused by applying traditional interdigital FEF sensor in the water tree detection. The mathematical model of the novel sensor is built by finite element method. Comparison of the electric field distribution that produced by the above two kinds of sensors is carried out by finite element analysis. Effect on novel sensor performance caused by excitation frequency is discussed. Parameters of the proposed sensor are optimized by analyzing the electric field penetrability with varying finger width and electrode separation. Simulation results demonstrate the sensor's design is reasonable and the electric field penetrability of the novel sensor is remarkably improved compared with traditional interdigital FEF sensor.**

***Index Terms*—insulation status, underground power cable, mobile monitoring, water tree, fringing electric field, interdigital sensor, finite element method**

I. INTRODUCTION

To ensure high quality and reliability of electric power supplied to customers, effective maintenance and monitoring of underground power cables is becoming one of the most significant tasks of today's power industry. Cross-linked polyethylene (XLPE) is used most widely in insulation material of cables, because of its excellent mechanical, thermal and electrical properties. After put into service, however, surrounding factors will affect serviceability and lifetime of cables. In order to ensure high quality of electric power supplied to customers, it is necessary to estimate the aging status of installed cables.

Existing cable maintenance practices include unplanned maintenance or planned maintenance [1]. Unplanned maintenance is a response to a failure that may have caused a fault in power delivery. Planned maintenance is a scheduled inspection or replacement of power cables. Although planned maintenance ultimately delivers a more reliable continuous service, it is not an economical option for utilities.

One of the primary causes of aging breakdown for XLPE cable is water tree [2], which may be formed in the insulation due to the combined effect of water and intense electric field. These trees typically develop from a small initial crack, void, or delaminated area. It takes several weeks to several years before the incipient fault causes cable failure. Various methods have been proposed for the diagnosis of water tree, such as DC leakage current method, residual charge method and insulation impedance method. All of these methods are all qualitative researches, which can not locate water tree in insulation layer accurately.

In literature [3, 11], a new and innovative mobile monitoring method is proposed to replace manual inspection. In this method, fringing electric field (FEF) sensor is applied to measure the presence of water in the bulk of the insulation. At present, most applications of fringing electric field dielectrometry method are on the monitoring of moisture concentration in transformer pressboard.

In this paper, a robotic monitoring system is described to complete the tasks of insulation status detection. A novel fringing electric field method is adopted in water tree detection. An arch substrate based interdigital FEF sensor is proposed to improve the accuracy of detection result. Its mathematical model is built by the finite element method. Effect on the novel sensor performance caused by various frequencies of driving voltage is analyzed by simulation results. We also discuss the effectiveness on electric field penetrability through finite element simulation, and optimize the sensor's parameters including the finger width and electrode separation.

II. THE MOBILE ROBOT

Insulation status mobile monitoring of underground power cables depends on a robot platform which can move along the underground power cables stably. We

doi:10.4304/jcp.8.2.441-447

have developed the robot platform with such function for insulation status mobile monitoring [4]. The framework of the robot platform, as shown in Fig. 1, is designed as a novel shrimp rover-based mobile robot. Hourglass-shaped wheels which located at both ends of the robot can keep the platform travel along the power cable. With help of the balance slide, which installed on the top of the robot, the platform can accomplish balance adjustment constantly while operate over large distances and climb over obstacles within the environment.

Insulation status mobile monitoring system is based on multi-sensor information fusion technology. The inspection subsystem of the robot platform includes four modules: overheating monitoring module, water tree detection module, partial discharge detection module, and video monitoring module. Infrared sensors in the overheating monitoring module do not need to contact with the cable, which can take intermittent measurements of temperature. The water tree detection and the partial discharge detection module are used to estimate the health status of power cables. The FEF sensor and acoustic sensor in modules need a proper contact with the cable surface to get accurate data. The video monitoring module can work continuously when the robot patrols the cable. Fig. 4 illustrates these operating modes. The quantity of data collected by each sensor is proportional to the height of the shaded areas. The information which collected by sensors in each module will be processed to estimates the status of insulation.

The inspection robot can perform monitoring tasks either autonomously or under remote control. When under autonomous mode, infrared sensors work continuously; take temperature readings as robot travels along the cable. If general scan detects a hot pot existing, the robot will stop and take more detail measurements. FEF sensor and acoustic sensor are driven down by a balanced mechanism to contact with cable surface. A force feedback control loop is employed to ensure proper force in the process, since small force can not guarantee adequate contact while excessive force may damage sensors and driving mechanism. While detection accomplished, sensors will be driven up, avoid affecting the robot climb the obstacles. Then sensor data will be saved in control board to make judgment on aging status. Within the communication distance, robot works under remotely operation, transmit information back to the host computer, and can be host to measure insulation status of appointed position.

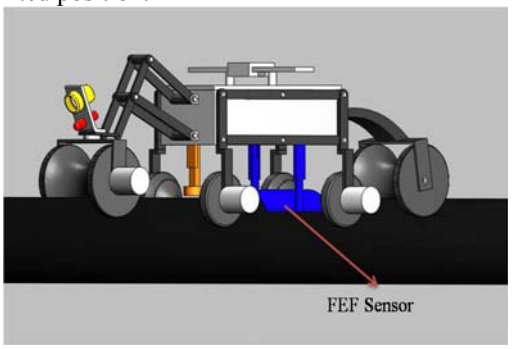

Figure 1. Shrimp rover-based mobile robot for status monitoring of underground power cables.

III. Water Tree Detection Module

The existence of water trees in insulation is the most common causes of partial discharge, which is the precursor to cable breakdown. The water tree detection module is installed on the robot to make continuous measurement of the cable surface and detect abnormalities in the insulation layer.

The performance of sensors will affect precision of insulation status monitoring. Diagnostic sensors in the modules are located on front end of the system. Due to the requirement for mobile monitoring and impact from the operating environment, sensors chosen for mobile monitoring system should meet following criteria: a) sensors must be able to make detection without destroying physical structure of cables; b) sensors must be small and lightweight that can be easily assembled into the platform; c) sensors must be have high precision that can make correct judgment in real-time; d) sensors must be sufficiently rugged that will not be damaged by the impact.

Fringing electric field method could be used as an effective way to measure the aging status of cable insulation layer in insulation status mobile monitoring. Since changes in the dielectric properties are usually induced by changes in various physical, chemical, or structural properties of samples, the dielectrometry measurements provide effective means for indirect nondestructive evaluation of parameters in a variety of scientific and industrial applications. In this method, dielectric properties of the insulation layer are associated with its physical characteristics. And the measurement of dielectric properties of outer layer can provide valuable insights into insulation status.

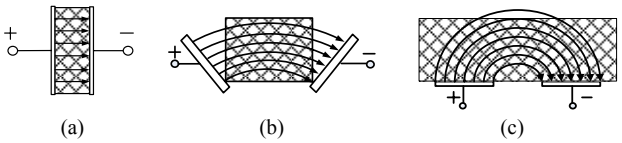

Figure 2. Gradual transition of a fringing electric field dielectrometry sensor from (a) a parallel-plate capacitor whose electrodes open up to provide (c) a one-sided access to the sample.

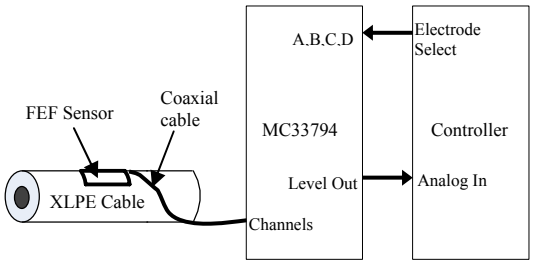

Figure 3. Circuit diagram of water tree detection module.

FEF dielectrometry sensor is a typical application of fringing electric field method. A FEF sensor can be visualized as a parallel-plate capacitor whose electrodes open up to provide one-sided access detection. Fig. 2 shows a gradual transition from the parallel-plate capacitor to a fringing field capacitor. In all three cases, electric

field lines pass through the sample; therefore, the capacitance and conductance between the two electrodes depends on the material dielectric properties as well as on the electrode and material geometry. This general principle allows design of sensors for a very broad spectrum of applications including relating changes in electrical properties to physical properties such as moisture, temperature, density, defects [5].

In order to build up an easily measurable electrode structure, the coplanar strips pattern could be repeated several times, which is called interdigital electrode. The interdigital electrode enlarges capacitance of the FEF sensor, improves the electric field distributing, so that it can guarantee better accuracy in the inspection.

The generic FEF sensor contact with arc surface lack-of-fit. In the task, the monitoring target of the mobile robot is the underground power cable, which with circular cross section. When temperature and humidity change, the variety of atmosphere dielectric property will disturb the detection results. A novel arch substrate based interdigital FEF sensor is designed to overcome this problem. The novel sensor reduces the gap between sensor and cable surface, and provide contact region as large as possible in the detection.

The introduction of Electric-field IC chip MC33794 makes it feasible to put an interdigital FEF sensor on the mobile monitoring platform. Fig. 3 shows the schematics of the water tree detection module, which is capable of broadband frequency and multi-channel sensing. When connected to external electrodes, the chip creates an electric field and generates a low-frequency sine wave. The frequency is adjustable by using an external resistor and is optimized for 120 kHz.

The growth of water trees causes an increase of the electric conductivity, permittivity and dielectric losses in insulations [6, 7]. In the process of monitoring, the existence of water tree will cause variety of the capacitance between the driving and the sensing electrodes. The capacitance can be converted into voltage by the E-field chip. After the data transmitted, the controller will achieve the variety of the capacitance accurately. Judgment for aging status of the insulation layer can be accomplished in short time.

IV. MODELING

A. Traditional FEF Sensor

A traditional interdigital FEF sensor, which used for nondestructive detection, is presented in Fig. 4. The driving and the sensing electrodes are designed as coplanar fingerlike pattern that repeated several times. Due to its space structure, the sensor produces periodic varietal electric potential difference in the *x* direction, and forms the spatial waveform. The electric field distribution is assumed uniform in the *y* direction. And the sensor forms approximate equipotential plane in the *z* direction. When the distance between the plane and the sensor increases, the electric field intensity decreases gradually. The penetration of fringing quasi-static electric fields above the interdigital electrodes is proportional to the spacing between the centerlines of sensing and driven fingers.

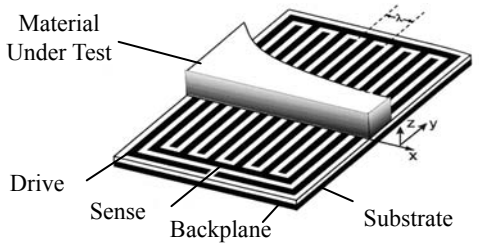

Figure 4. Schematic diagram of interdigital FEF sensor detection [8].

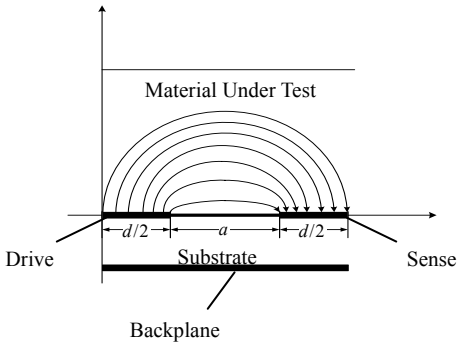

Figure 5. The simplified model for traditional interdigital FEF sensor.

The field intensity and its distributing are associated with the input voltage and electrode geometry. The backplane is used to eliminate induced current flows across the substrate between the driving and the sensing electrodes. The voltage of backplane should be kept at the same value with the sensing electrode.

The spatial wavelength of the periodic interdigital structure is the distance between the centerlines of the adjacent fingers belonging to the same electrode. And it is twice breadth of the electrodes centre distance. When the driving electrode is connected to an alternating voltage source, the sensor will produces fringing electric field.

In order to solve the approximate capacitance between normal interdigital electrodes conveniently, edge effect in long direction is ignored. Electric field lines between two contiguous fingers are supposed as circular curve or ellipse curve. The capacitance of the line element electrodes is considered in the first. We can build the simplified model of the generic sensor as Fig. 5 shows, the unit area obtained in the following way:

$$\Delta S = L \cdot \Delta x \,. \tag{1}$$

where Δx is the increment in width, L is length of electrode fingers. The capacitance of unit area can be calculated:

$$\Delta C \approx \frac{\varepsilon_x \cdot \Delta S}{\pi(x + a/2)} = \frac{2 \cdot L \cdot \varepsilon_x}{\pi(2x + a)} \Delta x \,. \tag{2}$$

where a is the separation of fingers, L is the length of the electrode, x is the length variable in width, ε_x is the permittivity of material under test. Regard the electrode

width as summation of line element electrodes, the capacitance can be integral from 0 to $d/2$, where d is width of a finger. The approximate expression of traditional interdigital FEF sensor is obtained by integration:

$$C \approx n\int_0^{d/2} \frac{2\cdot L\cdot \varepsilon_x}{\pi(2x+a)}dx = \frac{2\cdot n\cdot L\cdot \varepsilon_x}{\pi}\int_0^{d/2}\frac{1}{(2x+a)}dx = \frac{n\cdot L}{\pi}\ln(\frac{d+a}{a})\varepsilon_x . \quad (3)$$

where n is the number of the finger.

B. Novel FEF Sensor

Novel FEF sensor is based on arch substrate, which is designed to improve the surface contact quality. In modeling of the novel FEF sensor, it lacks of characteristic and geometrical features of cable insulation. Thus, 2D electric field distribution model is not convenient to express surface capacitance of the novel sensor [9]. We can calculate the potential distribution of the novel sensor follow the law of charge conservation.

Finite element method (FEM) is used extenstively for sensor modeling, optimization, and performance evaluation, especially for structures that are difficult to model analytically [10]. FEM is based on the idea of partitioning bounded domains in into a number of small, non-overlapping subdomains, the finite elements. After the scalar potential distribution is figured out by FEM, electric charge quantity on sensing electrode can be calculated. If it is known quantity of the potential difference between driven and the sensing, the capacitor can be calculated in the following way:

$$C = \frac{Q}{U}. \quad (4)$$

When the space is assumed without free charge, the sensor model based on Poisson equation:

$$\nabla[\varepsilon_0\varepsilon(x,y)\nabla\phi(x,y)] = 0 . \quad (5)$$

is satisfied everywhere in the space. In this equation, ε_0 is the permittivity of vacuum, $\varepsilon(x, y)$ is the relative permittivity distribution on cross section of sensor, (x, y) is electric potential distribution. As division element shown in Fig. 6, the potential distribution can be obtained as follows:

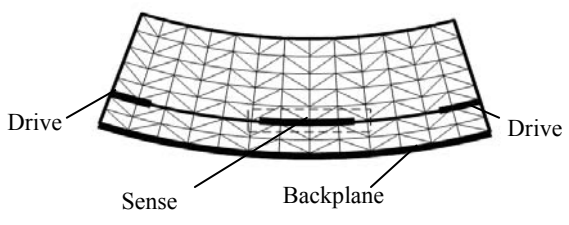

Figure 6. The simplified model for novel interdigital FEF sensor

$$\phi = \frac{\varepsilon(x,y)}{2S}[\sum_{p=1}^{3}(a_p + b_p x + c_p y)\phi_p] . \quad (6)$$

where a_p, b_p, c_p are the coefficient depending on vertex of triangle element, and p is the electric potential of vertex. From the electromagnetic field theory, we obtain:

$$E(x,y) = -\nabla\phi(x,y) . \quad (7)$$

By Gauss theorem, we obtain electric charge quantity on sensing electrode:

$$Q = \int_\Gamma \varepsilon_0\varepsilon(x,y)Eds = -\int_\Gamma \varepsilon_0\varepsilon(x,y)\nabla\phi(x,y)ds . \quad (8)$$

where Γ is the camber surrounding the sensing. Assume N is the number of electrodes in the array, we substitute (8) into (4) to yield, then:

$$C = N\frac{Q}{U} = -\frac{N\varepsilon_0}{U}\int_\Gamma \varepsilon(x,y)\nabla\phi(x,y)ds \quad (9)$$

V. Finite Element Simulation

A. Simulation Setup

The Maxwell finite element method software package by Ansoft Corp. is used for calculation of electrical field distribution and capacitance. Electrical field is assumed uniform along the surface in the y direction in the Fig. 4. Therefore, entire field distribution can be obtained through analyzing the cross section which perpendicular to the y direction.

2D AC Conduction Field Solver is applied to solve the sensor model. Draw the idealized model at Cartesian coordinate in the first. Then the material of the insulation layer is set to XLPE, which is valued with dielectric constant 2.3 and conductivity 10^{-8}S/m. Material of electrodes and substrate are set respectively to copper and Teflon. The driven electrode is held at 5V peak sinusoidal excitation, and the sensing electrode and the backplane are connected to ground. After the automatic elements distribution accomplished, the entire area is superimposed meshed with triangular finite elements. The density of finite elements is higher in the regions near the electrodes. Generally, a denser mesh results in a more accurate solution; however, it is also more computationally expensive.

B. Comparisons

The simulation results of equipotential lines in the insulation layer, which caused by sensors with varied substrate shape, are shown in Fig. 7. Obviously, the equipotential line produced by the traditional sensor is almost parallel to plane. The two driving fingers close to the cable surface have better penetration capability, while the outside fingers lead to the electric field mostly in the air between the sensor and the cable surface, with weaker penetration capability.

In Fig. 8 shows equipotential lines produced by the novel interdigital FEF sensor. We can get observation that four fingers of the driving electrode posses approximately equal penetration capabilities. Equipotential lines which

around sensing fingers are in sharper shape, and are denser in the insulation layer. Meanwhile, equipotential lines along the edge of the novel sensor have uptrend with a certain degree arch. Thus, covering area of the electric field expands, which results in more accurate detection results.

The strength variation in the insulation layer, which produced by the novel sensor, is compared with which produced by the traditional FEF sensor. After solving

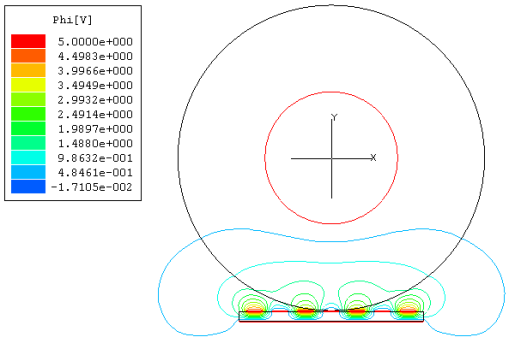

Figure 7. Equipotential line in insulation layer produced by a traditional FEF sensor.

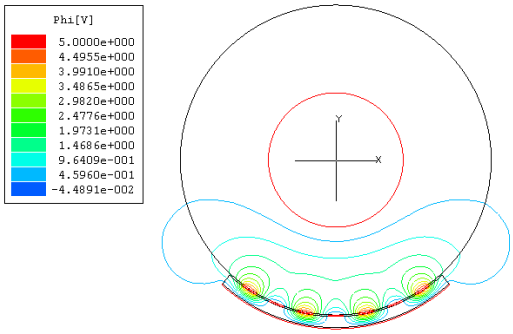

Figure 8. Equipotential line in insulation layer produced by a novel FEF sensor.

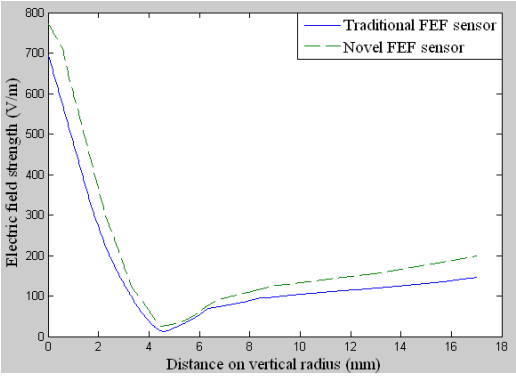

Figure 9. The potential along the cable radius perpendicular produced by the traditional and novel FEF sensors.

electric field strength by Maxwell, we fit the data at a coordinate with MATLAB, as shown in Fig. 9. The x-coordinate is the distance to the sensor surface in vertical direction. We can see that electric field strength of the novel sensor is 770 V/m on the sensor surface, where the traditional one is 690 V/m. And field strength of the novel sensor is higher at every points of the equal distance. Relative to the generic FEF sensor, the novel FEF sensor has a slower attenuation rate. Electric field strength of two sensors degrades rapidly away from the sensor surface. Due to existence of the cable core, field strength increase at the place where is 4mm to 5mm from sensor surface.

C. *Effect of Excitation Frequency*

Discussion on the effect to electric field distribution caused by variety of excitation frequency is important to the design of water tree detection module. In the finite element simulation, thickness of the electrode is not negligible, thus, air gaps exist between the cable surface and the substrate.

By comparing Fig.10 and Fig.11, which show the partial equipotential lines separately with the excitation frequency of 5Hz and 100Hz, we can see that electric field exist in three parts: the insulation layer, the sensor substrate and the air gap. In both cases, the electric field intensity in the gap between the backplane and sensing electrodes is very low because they are at the same potential.

In Fig. 10, with the excitation frequency of 5 Hz, the equipotential lines in the insulation layer come perpendicularly from above to the XLPE-air gap interface, while lines slope to left slightly with the excitation frequency of 100 Hz shown in Fig. 11. The equipotential lines which in the substrate has smaller angles between air gap-Teflon interface and themselves in the case of low frequency. And it is the similar case on the lines in the air gap. In the high frequency case, the normal component of displacement field is almost continuous across the interfaces because both materials (XLPE, air and Teflon substrate) appear to be insulating. This happens because the conduction currents at low frequency, in the water tree detection, are much higher than the capacitive currents.

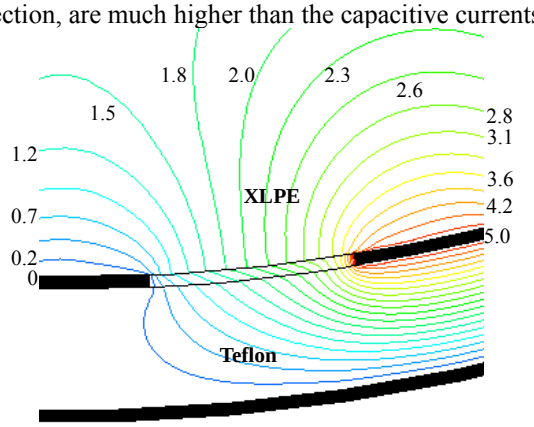

Figure 10. Equipotential lines at an excitation frequency of 5Hz in the half-wavelength section of the novel FEF sensor.

In Fig. 11, the equipotential line at the same potential can penetrate to deeper place in the insulation layer. Simulation results indicate that the novel sensor with the higher excitation frequency has denser electric field distribution, and has a better penetration capability.

Fig. 12 shows the calculated distribution of the electric potential along the cable radius that perpendicular to the driving finger with different excitation frequencies. One

can see that the slope of the potential is higher near the electrodes, which corresponds to higher intensity of the tangential electric field. At frequencies of 0.1 Hz and 1 Hz, the potential near the electrodes rise rapidly when frequency rise. The potential have no significant change after frequency reaches 4 Hz.

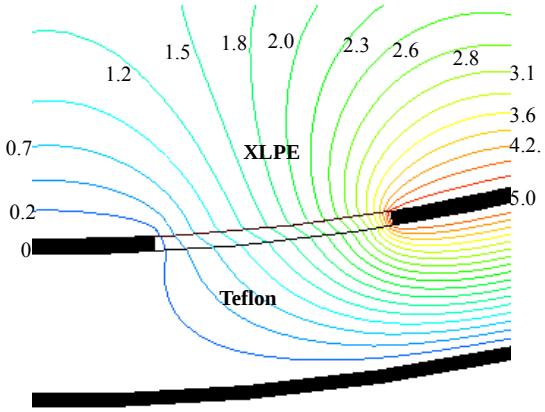

Figure 11. Equipotential lines at an excitation frequency of 100Hz in the half-wavelength section of the novel FEF sensor.

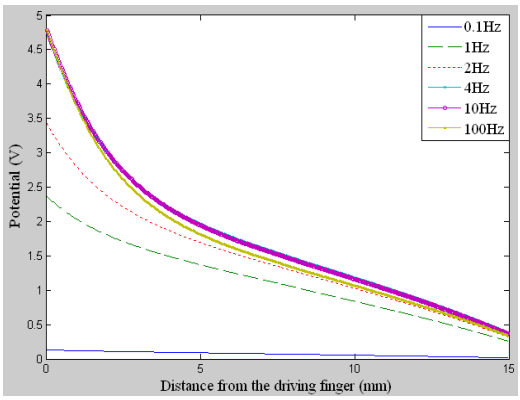

Figure 12. Distribution of the potential along the cable radius perpendicular to the driving finger with different excitation frequency.

VI. PARAMETER OPTIMIZATION

In order to conduct further research into effect of the novel FEF sensor in water tree detection of cables, electrode separations and finger widths are varied respectively. Effectiveness of the electric field penetrability is analyzed with FEM simulation, which leads to the optimization of parameters.

Keeping finger width as 3mm, sensors with separation constant 2.0, 2.5, 3.0, 3.5, 4.0mm are chosen for simulation and obtained respective electric potential strength on the circumference of the circle with radius 23mm. Curves of electric potential and field density are shown in Fig.13. We can see from the plot that with separation increases, the maximum value of electric potential on that circumference decreases gradually, whereas covering area of electric field expands. Four peaks appear in each curve, because the driving electrode has four fingers, and the amplitude of fluctuation increase with separation increases.

The electric field strength curves on the vertical radius caused by varied separations are shown in the Fig. 14. On the XLPE-sensor interface, the magnitude of the electric field strength decreases as separation increases, while attenuation speed slows down.

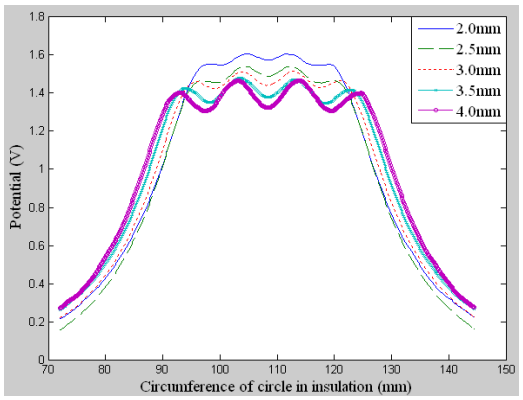

Figure 13. Electric potential and field density curves with variation of electrode separation.

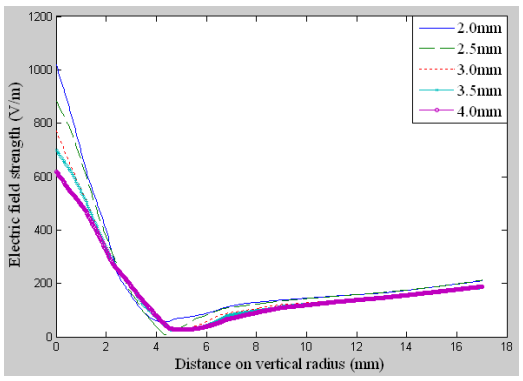

Figure 14. Electric field strength curves with variation of electrode separation.

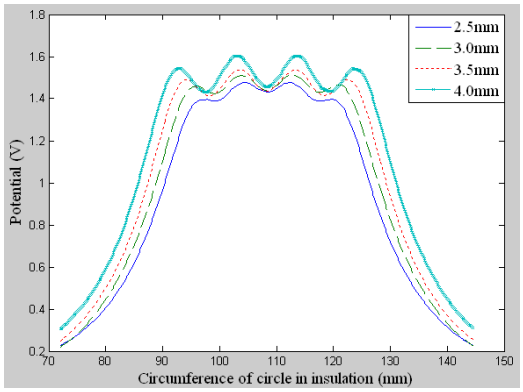

Figure 15. Electric potential and field density curves with variation of finger width.

Keeping separation as 3mm, sensors with finger width 2.5, 3.0, 3.5, 4.0mm are chosen for simulation and obtained respective electric potential strength on the circumference of the circle in the cable insulation layer with radius 23mm. Curves presented in Fig. 15 shows, while finger width increases, magnitude of electric potential on the circumference increases, the covering area of electric field grows as well; hence, the penetrating capability of sensor augments. And the amplitude of four peaks increases with finger width decreases.

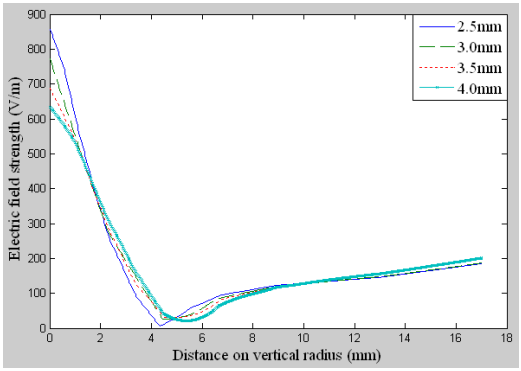

Figure 16. Electric field strength curves with variation of electrode finger width.

The electric field strength curves on the vertical radius caused by varied finger widths are shown in the Fig. 16. On the XLPE-sensor interface, field strength decreases as finger width increases, while attenuation speed slows down gradually. Due to the demand that the size of the sensor should be small enough in the mobile monitoring, the finger width is limited in a certain degree. Based on available area of practical application, we should pick inter-digital electrodes with the largest possible finger width.

VII. Conclution

This paper designed a novel interdigital FEF sensor to provide an innovative way for insulation status measurement. By finite element simulation, the electric potential and the field distributing are analyzed to compare the novel FEF sensor with the traditional sensor. And it is proved that the novel sensor is superior in water tree detection since it contact cable surface tightly. Parameters including finger width and electrode separation are optimized in simulation, which will instruct the physical design of the proposed sensor and water tree detection experiment while applied in the developed robot platform in our future work.

References

[1] B. Jiang, A. P. Sample, R. M. Wistort, and A. V. Mamishev, "Autonomous robotic monitoring of underground cable systems," *Proceedings of International Conference on Advanced Robotics*, pp. 673–679, 2005.

[2] J. Y. Li, X. T. Zhao, G. L. Yin, and S. T. Li, "The effect of accelerated water tree ageing on the properties of XLPE cable insulation," IEEE *Transactions on Dielectrics and Electrical Insulation,* vol.18, pp.1562-1569, 2011

[3] B. Jiang, and A. V. Mamishev, "Robotic monitoring of power systems," *IEEE Transactions on Power Delivery*, vol.19, pp. 912–918, 2004.

[4] S. Y. Dian, T. Liu, Y. Liang, M. Y. Liang, and W. Zhen, "A novel shrimp rover-based mobile robot for monitoring tunnel power cables," *Proceedings of 2011 International Conference on Mechatronics and Automation*, pp. 887–892, August 2011.

[5] S. Sulaiman, A. Manut, and A. R. Nur Firaus, "Design, fabrication and testing of fringing electric field soil moisture sensor for wireless precision agriculture applications," Proceedings of International Conference on Information and Multimedia Technology, pp.513–516, 2009.

[6] P. V. Notingher, M. Plopeanu, S. Grigorescu, and C. Stancu "The influence of water trees on permittivity and loss factor of medium voltage cables polyethylene insulation," *Proceedings of International Conference on Solid Dielectrics,* pp.1–4, July 2010.

[7] C. Stancu, P. V. Notingher, and J. Castellon, "Computation of the electric field in cable insulation in the presence of water trees and space charge," *IEEE Transactions on Industry Applications,* vol.45, pp.30–43, 2009.

[8] A. V. Mamishev, S. R. Kishore, and F. Yang, "Interdigital sensors and transducers," *Proceedings of the IEEE*, pp. 808–845, May 2004.

[9] Q. Sun, T. M. Shi, and J. Liu, "The methods of capacitance calculation between the electrodes of sensor in ECT system," *China Instrumentation*, pp.72–75, 2009.

[10] X. B. Li, S. D. Larson, and A. V. Mamishev, "Design principles for multichannel fringing electric field sensors," *IEEE Sensor Journal,* pp.434–440, April 2006.

[11] D. Y. Chen, M. Z. Li, and G. B. Zheng, "Analysis and parameter optimizing of multi-electrode capacitance transducers based on finite element method in electrical capacitance tomography system," *Chinese Journal of Electron Devices*, vol.29, pp.427–43, 2006.

Songyi Dian was born in Hubei, China in 1972. He received the B.S and M.S degrees in control engineering from Sichuan University, China, in 1996 and 2002, respectively. He received his Ph.D. degree in nanomechanics engineering from Tohoku University, Japan, in 2009. Currently, he is an associate professor in the School of Electrical Engineering and Information Technology of Sichuan University. His main research fields are control theory and strategies, precision motion control, measurement technology and intelligent robots.

Mengyu Liang was born in Zhejiang, China in 1988. She received the B.S in automation from Sichuan University, China in 2010. Currently, she is a graduate student of detection technology and automatic equipment in Sichuan University. Her main research field is intelligent detection of power cable.

Bingwu Lou was born in Zhejiang, China in 1990. Currently, he is an undergraduate student of electrical engineering and the automation in Sichuan University. His research interest is testing technology of power cable.

Tao Liu was born in Guizhou, China in 1987. He received the B.S degree in Electronic Information Science and Technology from North University of China, in 2009. Currently, he is a graduate student of control theory and control engineering in Sichuan University. His main research field is intelligent robots